Efficacy of ZrB_2 –SiC matrix in protecting C fibers from oxidation in novel UHTCMC materials

D. Sciti*, L. Zoli

CNR-ISTEC, Institute of Science and Technology for Ceramics, Via Granarolo 64, I-48018 Faenza, Italy

ABSTRACT

A series of high density UHTCMC materials with Cf content varying between 40 and 65% was produced by slurry infiltration and hot pressing. The matrix of UHTC consisted in ZrB_2 – 10 vol% SiC or ZrB_2 – 40 vol% SiC. The SiC phase was added either as ceramic powder or through a polymer-derived ceramic PDC.

The sintered materials were characterized in terms of microstructural features, mechanical properties, and oxidation resistance at 1650 °C. Materials with nearly fully dense matrix and optimized infiltration of C_f preforms were found to possess the highest strength (240 MPa) and oxidation resistance. Materials with weak interface and higher porosity in the matrix showed higher toughness (up to 12 MPa $m^{0.5}$) but were more prone to oxidation and erosion.

Keywords: Carbon, ZrB_2, mechanical properties, oxidation resistance

1. Introduction

Carbon belongs to the materials with the highest temperature resistance, if kept in non-oxidising environment. Under this condition carbon does not sublimate until a temperature of 3700 °C is reached and can be used in technical applications up to 2800°C [1]. For this reason, C/C and C/SiC are the materials used for aero-engine parts, hot gas valve parts, thermal structures and thermal protection systems (TPSs). [1] SiC is able to offer protection against oxidation at least up to 1600°C in an oxygen-rich atmosphere, thanks to the development of a SiO_2 surface film, however at temperature >1600°C and in low-oxygen atmosphere it develops a substantial vapor pressure. As a matter of fact, the combination of temperature over 1800°C, chemically aggressive environments and rapid heating cooling is beyond the capabilities of current engineering materials.

In recent years, several researchers have proposed the use of ultra-refractory ceramic (UHTC) phases such as ZrB_2, HfB_2, ZrC, HfC and TaC as an alternative mean to protect C preforms from oxidation and erosion. The most common approach adopted is to enrich the composite matrix with UHTC phases (usually with addition of SiC particles) using the combination of different techniques such as: slurry infiltration and CVI [2] [3], PIP [4] [5] [6], PIP and CVI [7] [8] [9], reactive melt infiltration [10] [11]. Some of those authors studied the ablation behavior of C/C-UHTC composites and reported a notable increase of the erosion resistance when UHTCs phases are added to the C/C composites. [2] [3] The efficacy of a UHTC phase in protecting C_f was also demonstrated in our previous studies on the ablation behavior of C_f-ZrB_2 containing 45% of random chopped Cf. [12] An alternative approach is a surficial infiltration of C/C composites with ZrB_2-SiC mixture to obtain oxidation resistant coatings that were shown to resist to oxidation up to 1600°C in air. [13]

Overall, there is an increasing interest in improving the capability of current engineering materials to withstand harsh environmental conditions integrating ultra-refractory ceramic phases in different technological processes.

In this paper, we produced new composites, the so called UHTCMCs (Ultra-High Temperature Ceramic Matrix Composites) through infiltration of C_f preforms by ZrB_2-SiC slurries and consolidation by hot pressing method. [14] This approach has been already successfully utilized for processing UHTCMCs with SiC fibers [15] [16] or for processing C/SiC composite. [17] Two aspects are the focus of the present work:

- on one hand the ability of carbon fibers to impart flaw tolerance to the composites;

- on the other the capability of the ZrB_2-based matrix to impart self-healing properties to the composite, protecting the fibers from excessive degradation in oxidation environment at temperature >1600°C.

Two different matrix compositions are investigated: -ZrB_2 – 10% SiC, obtained by dispersion of the powder mixture into water or -ZrB_2 – 40% SiC, obtained through dispersion of ZrB_2 into a SiC polycarbosilane precursor. The fiber content ranged from 40 to 65%. Flexural strength and fracture toughness were measured and discussed in relation with fiber amount and fiber/matrix interface. The oxidation resistance was studied through thermal treatment at 1650°C, in air, for 1 min in a bottom loading air furnace. The efficacy of the matrix to protect the fiber was investigated in terms of fiber/matrix interface, amount of UHTC phase, robustness of the interface.

2. Experimental

The following raw materials were used: -ZrB_2 (Grade B, H.C. Starck, Germany), specific surface area 1.0 m^2/g, particle size range 0.5-6 µm, impurities (wt. %): 0.25 C, 2.00 O, 0.25 N, 0.10 Fe, 0.20 Hf; -Alpha SiC (Grade UF-25, H.C. Starck, Germany) specific surface area 23-26 m^2/g, D_{50} 0.45 µm; allyl-hydride-polycarbosilane (SMP-10, starfire system Inc. U.S.A.), density 0.998 g/cm^3, as SiC precursor; commercial high modulus pitch-derived C_f preforms were used.

For the matrix of UHTCMCs, a ZrB_2 -10 vol% SiC powder mixture was preliminary prepared by wet ball milling and drying. With this mixture, aqueous slurries were prepared according to previous studies [18] using polyacrylates at different molecular weight as dispersants to tailor the fiber volumetric amount. Neither details about the dispersants nor characteristics of the slurries in terms of viscosity are intentionally indicated in this work. The composites were fabricated infiltrating the 1-D fabrics with the slurries by hand lay-up and subsequently stacking 8 layers in a 0-90° configuration. For all the compositions, vacuum-bagging was used to remove air bubbles entrapped in the green composite and to line up the fibers. Hot pressing cycles were then carried out in the range 1800 -1900°C, using a pressure of 30-40 MPa, on the basis of previous studies. [13]

In parallel, a series of composites were prepared by the same procedure shown above but directly dispersing the ZrB_2 particles into a liquid allyl-hydride-polycarbosilane instead of an aqueous solution. The curing of the polycarbosilane was performed in vacuum bagging at 150°C for 1h, after that the pellet was thermally treated (pyrolysis) under argon flux at 800°C for 30 min in graphite furnace and then hot pressed at the same conditions reported above.

The microstructures were analysed on polished and fractured surfaces by field emission scanning electron microscopy (FE-SEM, Carl Zeiss Sigma NTS Gmbh Öberkochen, Germany) and energy dispersive X-ray spectroscopy (EDS, INCA Energy 300, Oxford instruments, UK). X-ray diffraction Bruker D8 Advance apparatus (Bruker, Karlsruhe, Germany).

The starting compositions (e.g. the fiber and matrix volumetric amounts) were estimated in different steps. Before sintering, the green pellet was weighted and the fiber volumetric amount was determined considering the fabric weight (g/m^2) given by the supplier, number of layers and sample area. The matrix

amount was then determined after debonding by subtraction of the total pellet weight minus the fiber weight. Hence, a theoretical density of the materials based on the initial composition was calculated using the rule of mixture. After sintering, the bulk density was determined by the Archimede method. The relative density, ρ was thus calculated as the ratio of experimental to theoretical value, and the residual porosity deduced as 1-ρ.

For samples in which SiC is added as polymeric precursor, Image analysis (Image- pro analized 7.0) carried out onto SEM micrographs of polished sintered sections allowed to determine the amounts of as-obtained SiC, C_f and porosity (see values in Table 1).

As for the mechanical properties, 4-pt bending strength tests were carried out for selected compositions. The test bars, 25 x 2.5 x 2 mm^3 (length by width by thickness, respectively) were fractured using a semi-articulated silicon carbide four-point fixture with a lower span of 20 mm and an upper span of 10 mm using a screw-driven load frame (Instron mod. 6025, Instron, High Wycombe, GB). For each material at least four bars were tested. The fracture toughness (K_{Ic}) was evaluated by fracturing chevron notched beams (CNB). The test bars were 25 mm x 2 mm x 2.5 mm^3 (length by width by thickness, respectively) were notched with a 0.1 mm-thick diamond saw; the chevron-notch tip depth and average side length were about 0.12 and 0.80 of the bar thickness, respectively. The specimens were fractured using a fully-articulated steel four-point fixture with a lower span of 20 mm and an upper span of 10 mm using a screw-driven load frame (Instron, 6025). Three specimens were loaded with a crosshead speed of 0.05 mm/min. The “slice model” equation of Munz et al. [19] was used to calculate K_{Ic}. A bottom loading furnace was used to test the resistance to oxidation of the composites. This furnace allows introducing the samples when the test temperature is reached. This is particularly useful to avoid oxidation of the samples during the heating step. Once introduced in the furnace chamber, 30 s are necessary to reach the thermal equilibrium, then the short isothermal stage begins (1 min). After the end of the oxidation stage, the furnace is opened again, the samples removed and naturally air quenched.

3. Results and discussion

3.1 Microstructural features

Compositions, sintering cycles, fiber amount and densities of the composites are reported in Table 1. Polished sections of the composites are shown in Figure 1. According to the described procedure the starting compositions are:

1) 35% (90% ZrB_2 + 10% SiC) + 65% Cf, labelled as Z10S-65F;
2) 45% (90% ZrB_2 + 10% SiC) + 55% Cf, labelled as Z10S-55F;
3) 60% (90% ZrB_2 + 10% SiC) + 40% Cf, labelled as Z10S-40F;
4) 45% (60% ZrB_2 + 40% SiC) + 55% Cf, labelled as Z40S-55F.

Sample Z10S-65F, with (ZrB_2-10% SiC) as matrix and 65% of Cf has a bulk density of 2.9 g/cm^3 and a porosity around 15%. The laminate structure in Figure 1a, shows that the layers have approximate thickness of 200 µm. The infiltration is not complete, especially in the central area of the bundle. The incomplete densification of the matrix as well as intra bundle voids contribute to the total amount of porosity. Typical defects of these composites are: non-infiltrated areas and cracks in matrix-rich regions. Cracks originate for constrained shrinkage of the matrix during sintering and thermal expansion coefficient mismatch between matrix and fibers (6.5 10^{-6} °C^{-1}, [20] 2 10^{-6} °C^{-1}, [1] respectively). As for the matrix/fiber interface, a good adhesion was found but no reaction occurred, at least according to the SEM resolution (Figure 2a). Fracture surfaces (Figure 3a) show both bundle pull-out and individual pull-out. These features suggest a fiber – matrix debonding mechanism. The extent of fiber pull-out is strictly related to the cohesion between matrix and fibers that develops during the densification process.

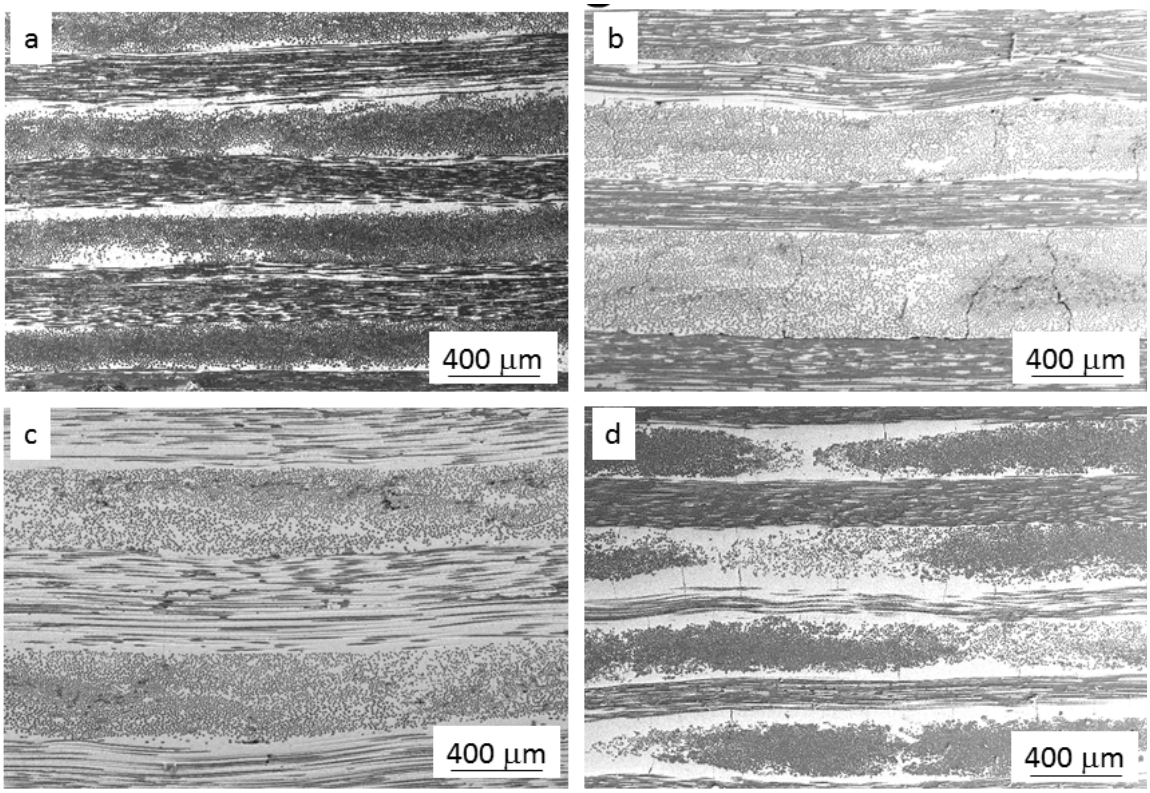

Figure 1: Polished section of samples: a) Z10S-65F; b) Z10S-55F; c) Z10S-40F; d) Z40S-55F.

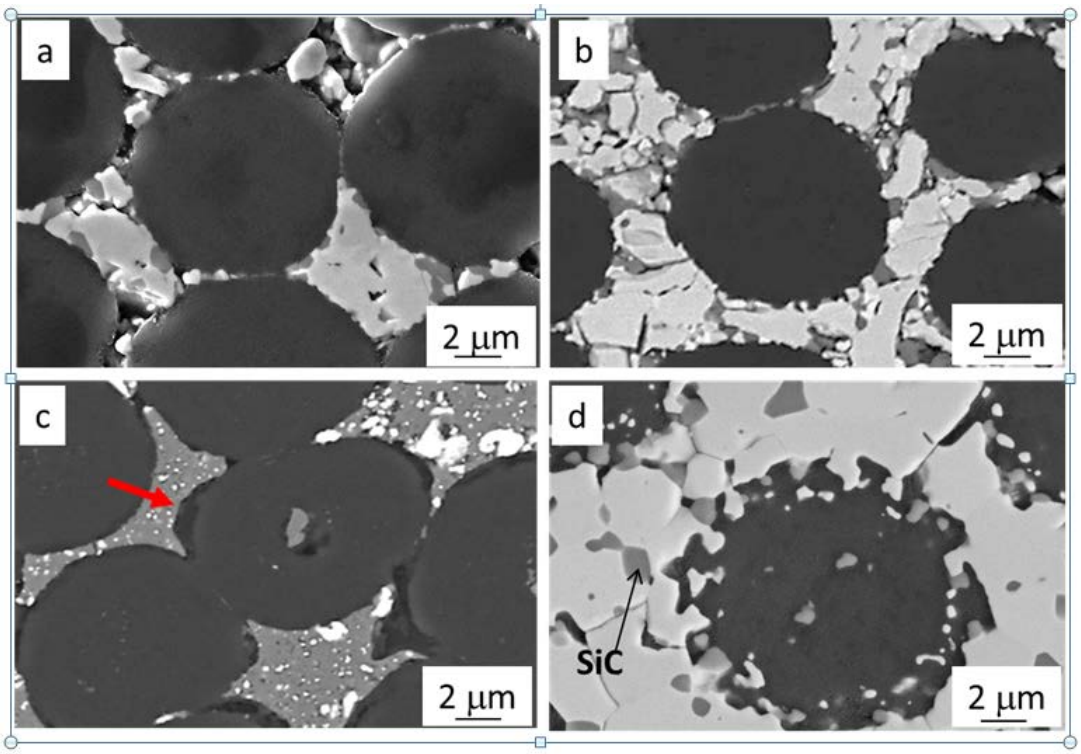

Figure 2: Details of the matrix-fiber interface for samples: a) Z10S-65F; b) Z10S-55F, c) Z40S-55F at the C/SiC interface and d) at the C/ZrB_2 interface.

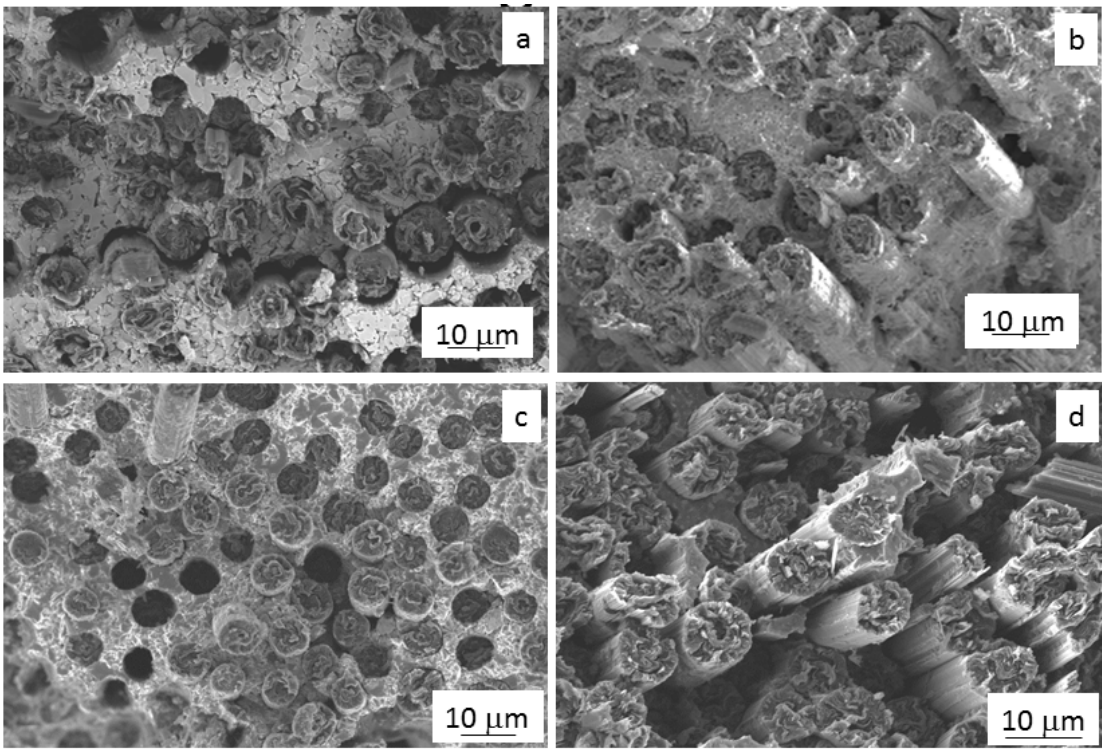

Figure 3: Fracture surfaces showing pull-out for sample a) Z10S-65F; b) Z10S-55F; c) Z10S-45F; d) Z40S-55F.

Sample Z10S-55F: This composite with a (ZrB_2-10% SiC) matrix and 55% C_f has a bulk density of 3.3 g/cm^3 and a residual porosity of 11% , Table 1. Tailoring the slurry viscosity allowed a very good degree of infiltration inside the fiber bundles by the matrix. Due to enhanced penetration of the slurry, the thickness of each individual layer is higher than the previous case, 300-400 µm, Figure 1b. Typical defects of this composite are transverse cracks due to tensile stress in the matrix and delaminations (not shown). As for the previous case, the extent of matrix – fiber reaction is very limited (Figure 2b) and this facilitates the fiber pull-out during fracture (Figure 3b).

Sample Z10S-40F: This composite with a (ZrB_2-10% SiC) matrix and 40% C_f has an even higher density, 3.9 g/cm^3, with a residual porosity around 8%. The typical layer thickness is >400 µm, Figure 1c. The higher density is due to both the lower content of fiber and the better level of matrix densification. Due to high homogeneity of the infiltration, the amount of cracks and delaminations is reduced compared to the previous samples. On the other hand, the better degree of densification even in the intra-bundle region, seems to reduce the extent of fiber pull-out compared to the other samples (see an example in Figure 3a) probably due to enhanced adhesion of the fiber to the matrix.

Sample Z40S-55F: The composite with a (ZrB_2-40% SiC) matrix and 55% C_f has a bulk density of 3.3 g/cm^3 and residual porosity lower than 5%, Table 1. Looking at the microstructure in detail, it can be seen that the tows are generally completely infiltrated, but in the central regions they are prevalently infiltrated by the polycarbosilane, whilst towards the border of the bundles, ZrB_2 is the major constituent phase. Two different interfaces are thus created for this composite: one intra-bundle C/SiC interface and an inter-bundle ZrB_2/SiC interface, see Figure 2 c,d. The C/SiC interface is relatively smooth (Figure 2c), and partial detachment of the SiC phase from the C_f is often observed (red arrow inset of Figure 2c). According to previous works on C/SiCN minicomposites [21] we hypothesize that these defects are due to the shrinkage occurring during pyrolysis of polycarbosilane. On the contrary, for carbon fibers embedded into the ZrB_2 matrix, a reaction layer developed and a clear grain interlocking between ZrB_2 and C_f was observed (Figure 2d). The fiber profile became jagged and SiC particles were recognized (see EDS) as observed in previous work [22]. As a consequence, the fiber pull-out was more pronounced in the C/SiC interface, but less pronounced in the reacted fiber/matrix interfaces (see Figure 3d).

3.2 Mechanical behavior

As previously mentioned, sample bars for mechanical testing were machined from the sintered pellets by diamond tool machining. The flexural strength of the four UHTC-composites ranges from 120 to 240 MPa. The values obtained are in agreement with those reported in the literature: H. Hu in [4] reported a flexural strength of 163 MPa for a C/SiC material enriched with about 25% of ZrB_2, Q. Li [5] reported a bending stress of 248 MPa for a 3D-C/SiC enriched with 23% of ZrB_2-ZrC phases, L. Li [8] found a value of 255 MPa for 2D-C/SiC enriched with a ZrB_2-TaC mixture.

The flexural strength does not increase with increasing the amount of fiber, in contrast with findings in the literature [17]. Indeed, samples Z10S-65F, Z10S-55F, Z40S-55F, with higher fiber content, 65 and 55%, have lower strength (120÷150 MPa) than the composite with the lowest content of fibers, Z10S-40F, e.g. 40% and 240 MPa. Flexural strength of these composites seems to be affected by other factors:

-the localized damage due the machining of the bars, that introduced surface defects, scratches in the fiber; furthermore due to the non-perfect alignment of laminate planes, the machined bar surface can be a patchwork of areas with fibers parallel and perpendicular to the loading direction;

-the content of fibers in the axial/transverse direction can vary between different bars;

-the presence of shear stresses due to non-optimized ratio between span and bar thickness.

As a result, a large data dispersion is observed especially for composites Z10S-65F, Z10S-55F (23-28%).

The fracture toughness measured through CNB in flexure, ranged from 6.4±0.8 MPa $m^{0.5}$ of the most dense sample (Z10S-40F) to 10.6±1.6 MPa $m^{0.5}$ for sample Z40S-55F, in agreement with data reported in the literature on C/SiC/ZrB_2 [4] and C/ZrC composites [10]. A comparison of typical load/displacement curves recorded for the four samples is shown in Figure 4a, while the extent of fiber pull-out is reported in the optical pictures of Figure 4e. Again the toughness can be affected by several factors: for instance, the higher values found for samples Z10S-65F and Z10S-55F compared to Z10S-40F could be due to the higher amount of fibers for the former (65 and 55%, respectively) and the stronger interface of the latter (compare for instance the lower extent of fiber pull-out of this sample in Figure 4d, with respect to sample Z10S-65F in Figure 4b). The higher amount of fibers induces more residual stress in the matrix with consequent cracking and decrease of the matrix modulus, which applies for Z10S-65F and Z10S-55F. The decrease of the matrix modulus is also induced by the higher amount of porosity, which occurs for sample Z10S-65F; both these two factors positively affect the value of fracture toughness. Sample Z40S-55F has a markedly higher value of toughness, which is likely related to the characteristics of the fiber/matrix interface, in particular to the ability of the C/SiC interface to promote more fiber pull-out than a ZrB_2/C interface, see Figure 4e. An interesting feature of this sample is the correlation between the data of fracture toughness and the notch tip positioning, as observed in the post test optical analysis. Higher values of fracture toughness (>10 MPa $m^{0.5}$) were found when the tip was located inside the C_f bundle under compressive stresses and lower (<10 MPa $m^{0.5}$) when the tip was positioned in ZrB_2 -rich areas, under tensile stresses.

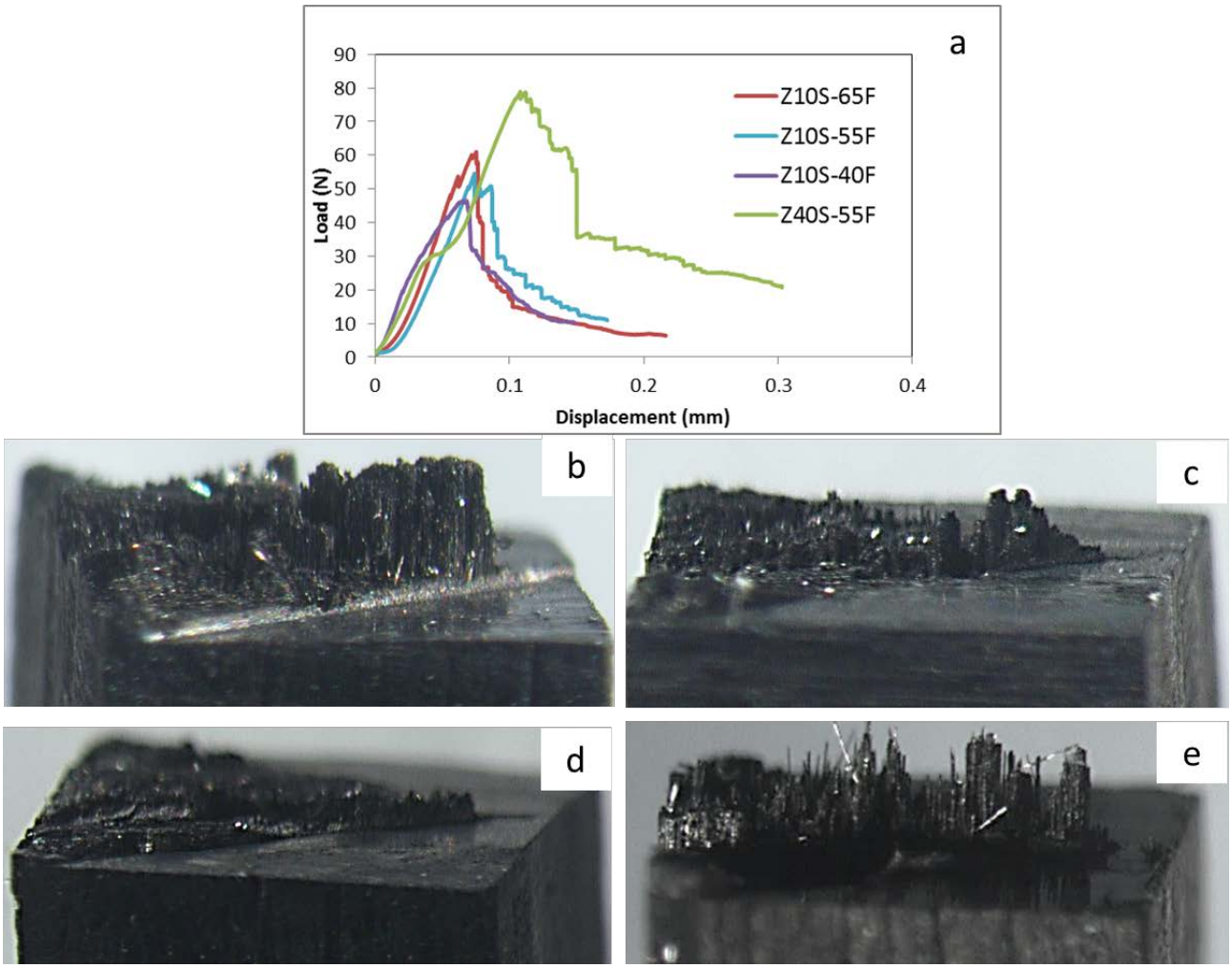

Figure 4: a) Comparison of load/displacement curves, b-e) the fracture surface of the notch after CNB tests for samples, b) Z10S-65F; c) Z10S-55F; d) Z10S-40F; e) Z40S-55F.

3.3 Oxidation behavior

All the samples were exposed to air at 1650°C, for 1 min. Figure 5 compares polished cross sections of samples Z10S-55F, Z10S-40F, Z40S-55F. The main phenomena occurring during exposition were oxidation of the matrix phases, e.g. ZrB_2 and SiC, and of the fibers according to:

$$ZrB_2 + {}^5/_2O_2(g) = ZrO_2 + B_2O_3(l) \quad (1)$$

$$SiC + {}^3/_2O_2(g) = SiO_2(l) + CO(g) \quad (2)$$

$$C + ½\ O_2(g) = CO(g) \quad (3)$$

ZrB_2 starts to oxidize at 600°C with formation of solid ZrO_2 and liquid B_2O_3 while carbon fibers start to vaporize significantly a T>700°C. The addition of SiC improves the oxidation resistance at temperatures above 1200°C by promoting the formation of a borosilicate layer, which reduces the oxygen permeability on exposed surfaces. The oxidation resistance was very different amongst the composites, being affected by a residual porosity, amount of C fibers, amount of SiC phase.

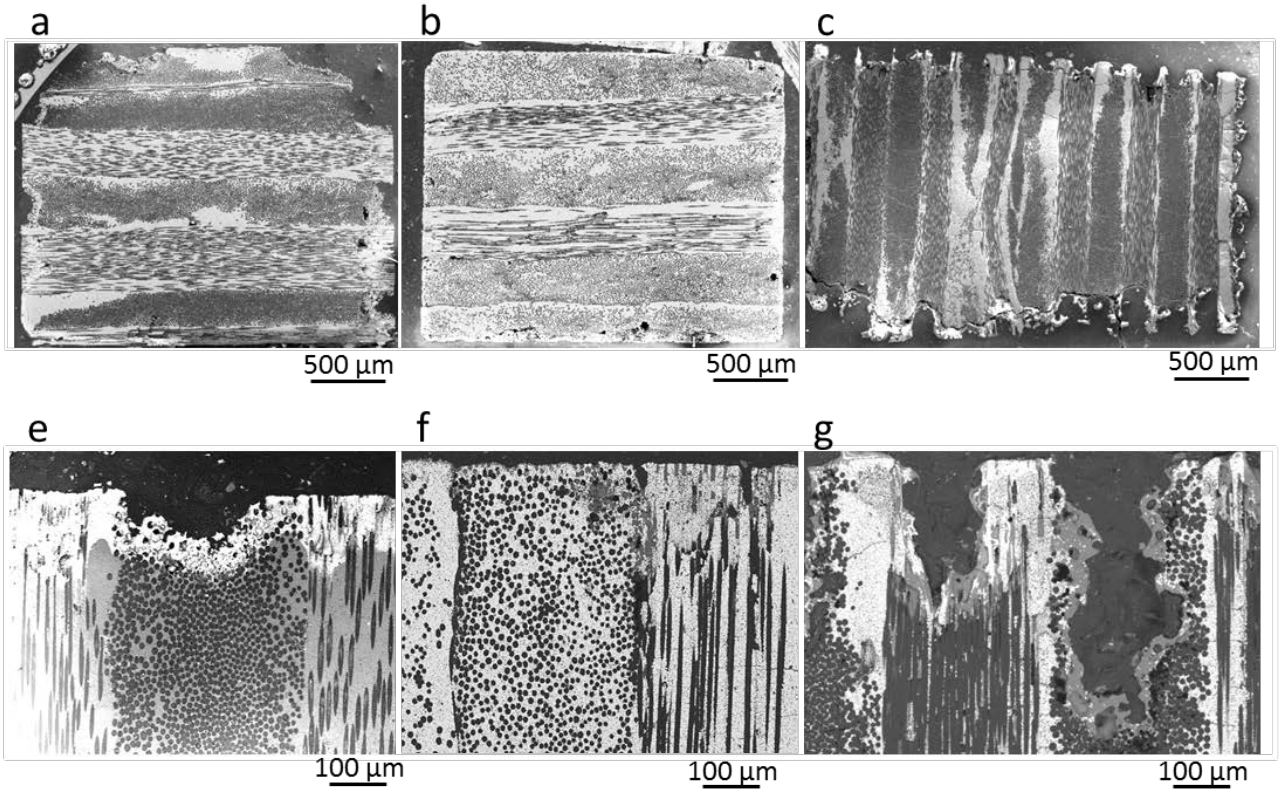

Figure 5: Oxidized cross sections (1 min at 1650°C) of samples, (a, e) Z10S-55F, (b, f) Z10-40F, (c, g) Z40S-55F.

Sample Z10S-65F with 65 % of C fibers was severely attacked by oxidation (not shown), due to the presence of a high amount of residual porosity and non-infiltrated intra-tow areas. Analysis of the surface confirmed that the oxygen penetrated in the voids of intra-bundle regions, causing fast vaporization of fibers and leaving a layer of porous ZrO_2. The sample cross section was difficult to prepare due to excessive brittleness.

Sample Z10S-55F, with nominally 55% of fibers showed a better resistance compared to previous sample, even if the oxidation and erosion affected the sample up to about 250 µm in depth. SiC addition

helped forming a somewhat discontinuous surface silica layer. Defective areas such as cracks, as well as intra-tow voids led to enhanced penetration of oxygen. On the section (Figure 5a, e) the scale profile was quite irregular, with more or less damaged/oxidized zones depending on local arrangements of fiber/matrix, presence of cracks or voids.

For **Sample Z10S-40F** containing 40% of carbon fibers, an almost continuous outer layer of silica was observed on the surface (Figure 5b, f). Exposure of these samples to air resulted in a layered morphology similar to what observed for ZrB_2-SiC composites containing graphite [23]. After exposition of 1 minute, the sample was topped by a non-continuous layer of SiO_2. Underneath this layer a ZrO_2-SiO_2 scale was found, where silica often replaced voids left by fiber evaporation. Below, C_f were immersed in a ZrO_2 scale until the unaffected bulk was reached. For this sample, the outer layer of ZrO_2 and silica could offer a significant protection to the carbon fibers. Moreover, voids left by evaporation of fiber located on/near the surface were partially filled with borosilicate phase diffusing towards the surface.

Sample Z40S-55F. An overview of the cross section reveals that this sample underwent a strong erosion, which was more marked in fiber-rich regions infiltrated with the SiC precursor (Figure 5c, g). Areas where the fibers were circumvented by the SiC phase were more eroded than areas where the fibers where circumvented by the ZrB_2 grains. This could be due to the different composition of the oxide scale formed: in ZrB_2-rich regions, a ZrO_2-rich layer with few silica filling the holes was observed. On the contrary, when SiC-rich areas were exposed the formation of SiO_2 was less efficient in protecting the C fibers from fast evaporation.

3. Discussion: factors affecting the capability of the UHTC matrix to protect the fibers

A strongly recommended functionality for materials to be used in extreme environments is self-healing capability and self-protection. For bulk ceramics, self-healing is intended to be the partial or complete sealing of cracks through a thermal treatment (also called crack-healing). Much more recently, a self-healing ability has been invoked for UHTCs ceramics when 10-20 vol% SiC-based phases are added to UHTCs matrices (e.g. ZrB_2 and HfB_2). Self-protection is induced by surface-oxidation which results in the formation of a compact protective borosilicate layer [24]. In the bulk, oxidation products can easily penetrate into defects and flaws, thus leading to cracks being blunted and healed.

For UHTCMCs to be operated in harsh aerospace environment, the self-healing /self-protection capability is reached only with the in situ external formation of adherent, ultra-refractory solid oxide scales, essentially the oxidation products of the UHTC matrices, and simultaneous filling of voids by a liquid oxidation product in the bulk.

Within the samples developed in the present work, only the composite with 40% of fibers, namely, Z10S-40F seems to partially display this capability. This is due to multiple factors:

I) due to optimized infiltration, all C fibers are circumvented by the protective ZrB_2 matrix;

II) the matrix has very low porosity (<10%)

III) an homogenous distribution of SiC phase is achieved in the ZrB_2 matrix;

IV) a good cohesion is found at the ZrB_2/C_f interface.

Factor I suggests that volumetric amount of protective UHTC phase must be appropriately calibrated: the requirement is that each individual fiber is surrounded by a shell of UHTC grains. This, in turn, affects the minimum fiber/fiber distance which is correlated with the mean UHTC particle diameter and mean fiber diameter respectively. In a simplified system containing just two phases, where D_f and D_p are the mean fiber diameter and mean particle diameter respectively, the minimum volumetric amount (V_{min}) of ceramic phase (ZrB_2), that allows individual fiber coating is given by:

$$V_{min}(x) = \frac{((1+x)^2 - \pi/4)}{(1+x)^2} \qquad (4)$$

Being $x=D_p/D_f$

In the present case, with a mean ZrB_2 diameter of 2.5 μm and mean fiber diameter of 10 μm, the maximum amount of fiber that can be individually coated by the ZrB_2 shell is about 50%. Indeed only Z10S-40F satisfies this criterium, whilst for samples Z10S-65F and Z10S-55F the amount of fibers (65 and 55%) is too high to have a uniform coating by ZrB_2 (overall: 31 and 40% respectively), resulting in poor resistance to oxidation. A minimum amount of 5% of SiC (overall) causes the formation of borosilicate glass that diffuse across the scale, closing ZrO_2 scale porosity as well as voids left by cracks or fiber evaporation. For lower content of SiC (as in Z10S-65F, where the total amount of SiC is ~3.5%), the oxide is too friable and tends to detach from the bulk.

A particular case is that of sample Z40S-55F in which the addition of SiC is obtained through a polycarbosilane. Being a liquid precursors, the fiber bundle is infiltrated much easier compared to the aqueous slurry containing particles and the fibers. However, oxidation tests confirm that a mixed ZrB_2-SiC phase is more efficient in protecting the carbon fiber than SiC alone, thus areas where the fibers are locally coated just by the SiC phase are strongly eroded during oxidation. The protective action of the ceramic phase is also jeopardized by the partial detachment of SiC from C fibers, occurring during pyrolysis. Voids are indeed preferred paths for the oxygen diffusion.

It is interesting to compare the performance of the four samples analyzed. To this aim, the plot of Figure 6 shows the relative amounts of ZrB_2, SiC, Cf and porosity (normalized values).

It can be clearly seen that going from sample Z10S-65F to Z10S-40F there is an increasing of ZrB_2 and decreasing the amount of C fibers and porosity. On one hand, sample Z10S-40F has the best oxidation resistance -due to low porosity, low cracking, calibrated amount of fibers - and the lowest fracture toughness - due to stronger interface and high matrix modulus. On the other hand, the partially porous ZrB_2-matrices in samples Z10S-65F and Z10S-55F lead to high values of fracture toughness due to both decrease of matrix Young's modulus and weak fiber/matrix interface, but presence of porosity jeopardizes the resistance to oxidation/erosion. The addition of the SiC-precursor generates an intra-bundle SiC/C interface, which increases the mechanical properties (fracture toughness) but SiC alone offers a worse protection for C fibers with respect to the ZrB_2-SiC mixture.

With the research conducted so far, a higher fracture toughness is achieved at the expenses of a worse oxidation resistance. If oxidation/erosion resistance is the primary requirements, suitable fiber content vs UHTC phase content, strong interfaces and dense matrices seem to be preferable.

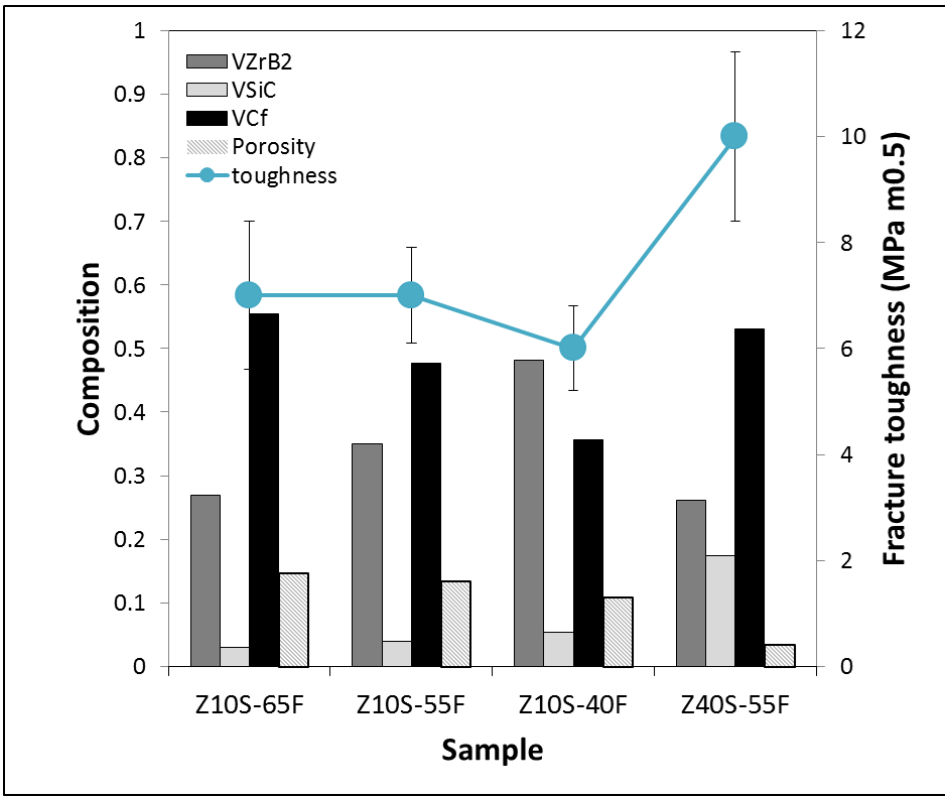

Figure 6: the plot shows the toughness and the relative amounts of ZrB_2, SiC, Cf and porosity (normalized values) of the four samples .

4. Conclusions

In this paper, we critically analyzed the performance of a novel UHTCMCs with variable C_f content (40 - 65%) and SiC phase content (10 and 40%), focusing on the capability of the UHTC matrix to protect the fibers from oxidation at 1650°C. We demonstrated that for an efficient protection the amount of fiber should not exceed the amount of protective matrix and that an efficient infiltration of the C preform by the protective matrix is necessary.

The research conducted also revealed that there is a trade-off between oxidation resistance and fracture toughness. A dense UHTC matrix is accompanied by a relatively strong ZrB_2-C_f interface offering a good oxidation protection but implying a lower value of fracture toughness. On the other hand, a partially porous ZrB_2-matrices leads to high values of fracture toughness due to both decrease of matrix Young's modulus and weak fiber/matrix interface, but presence for porosity jeopardizes the resistance to oxidation/erosion. The addition of SiC through a liquid precursor generates an intra-bundle SiC/C interface,

which increases the mechanical properties (fracture toughness) but SiC alone offers a worse protection for C fibers with respect to the ZrB_2-SiC mixture.

Acknowledgements

Authors wish to thank G. Angeloni srl for providing carbon fibers and preforms, D. Dalle Fabbriche and C. Melandri for technical support.

Table 1: Compositions, sintering cycles, fiber amount and densities of the composites

Label	Composition Vol%			Density (g/cm^3)	Porosity %	Flexural Strength (MPa)	CNB (MPa $m^{0.5}$)
	ZrB_2	SiC	Cf				
Z10S-65F	32	3	65	2.9	15	140±30 (24%)	7.5±1.4
Z10S-55F	38	5	57	3.3	12	125±35 (28%)	7.3±0.9
Z10S-40F	51	6	43	3.9	8	235±40 (18%)	6.4±0.8
Z40S-55F	27	18	55	3.3	4	152±12 (8%)	10.6±1.6

References

[1] W. Krenkel, Ceramic Matrix Composites: Fiber Reinforced Ceramics and their Application., Weinheim: Wiley-Vch. Verlag: Isbn: 978-3-527-31361-7, 2008.

[2] A. Paul, S. Venugopala, J. Binner, B. Vaidhyanathan, A. Heaton, P. Brown, «UHTC–carbon fibre composites: Preparation, oxyacetylene torch testing and characterization» *J Eur Ceram Soc*, n. 33, p. 423–432, 2013. doi:10.1016/j.jeurceramsoc.2012.08.018

[3] S. Tang , J. Deng, S. Wang, W. Liu, K. Yang, «Ablation behaviors of ultra-high temperature ceramic composites» *Mat Sci Eng A*, p. 465, 2007. doi:10.1016/j.msea.2007.02.040

[4] H. Hu, Q. Wang, . Z. Chen, C. Zhang, Y. Zhang, J. Wang, «Preparation and characterization of C/SiC-ZrB2 composites by precursor infiltration and pyrolysis process» *Ceram. Int.*, vol. 36, pp. 1011-16, 2010. doi:10.1016/j.ceramint.2009.11.015

[5] Q. Li , S. Dong, Z. Wang, G. Shi, «Fabrication and properties of 3-D Cf/ZrB2-ZrC-SiC composites via polymer infiltration and pyrolysis» *Ceram. Int.*, vol. 39, pp. 5937-41, 2013. doi:10.1016/j.ceramint.2012.11.074

[6] D. Zhao, C. Zhang, H. Hu, Y. Zhang, «Preparation and characterization of three-dimensional carbon fiber reinforced zirconium carbide composite by precursor infiltration and pyrolysis process» *Ceram Int*, vol. 37, pp. 2089-2093, 2011. doi:10.1016/j.ceramint.2011.02.024

[7] Y. Wang, W. Liu , L. Cheng, L. Zhang, «Preparation and properties of 2D C/ZrB2–SiC ultra high temperature ceramic composites» *Mater Sci Eng A*, vol. 524, p. 129–133, 2009. doi:10.1016/j.msea.2009.07.005

[8] L. Li , Y. Wang , L. Cheng, L. Zhang, «Preparation and properties of 2D C/SiC–ZrB2–TaC» *Ceramic international*, vol. 37, pp. 891-896, 2011. doi:10.1016/j.ceramint.2010.10.033

[9] . Z. Wang, S. Dong , X. Zhang, H. Zhou, D. Wu, Q. Zhou, D. Jiang, «Fabrication and properties of Cf/SiC-ZrC composites» *J Am Ceram Soc*, vol. 91, p. 3434–6, 2008. 10.1111/j.1551-2916.2008.02632.x

[10] S. Chen, C. Zhang, Y. Zhang, H. Hu, «Influence of pyrocarbon amount in C/C preform on the microstructure and properties of C/ZrC composites prepared via reactive melt infiltration» *Materials &*

Design, vol. 58, pp. 570-576, 2014. doi:10.1016/j.matdes.2013.12.071

[11] M. Kütemeyera, L. Schomera, T. Helmreichc, S. Rosiwalc, D. Koch, «Fabrication of ultra high temperature ceramic matrix composites using a reactive melt infiltration process» *Journal of the European Ceramic Society, in Press* 2016 doi:10.1016/j.jeurceramsoc.2016.04.039

[12] D. Sciti, L. Zoli, L. Silvestroni, A. Cecere, G.D. Di Martino, R. Savino Design, «fabrication and high velocity oxy-fuel torch tests of a Cf -ZrB2- fiber nozzle to evaluate its potential in rocket motors» *Materials & Design*, in Press 2016 doi:

[13] D. Sciti, A. N. Murri, V. Medri, L. Zoli, «Continuous C fibre composites with a porous ZrB2 Matrix» *Materials & Design*, vol. 85, pp. 127-134, 2015. doi:10.1016/j.matdes.2015.06.136

[14] L. S. Walker, E. L. Corral, «Self-generating High – Temperature Resistant Glass Ceramic Coatings for C-C composites using UHTCs» *J. Am. Ceram. Soc.*, pp. 1-8 , 2014. doi:10.1111/jace.13017

[15] L. Zoli, V. Medri, C. Melandri, D. Sciti, «Continuous SiC fibers-ZrB2 composites» *Journal of the European Ceramic Society*, vol. 35, p. 4371–4376, 2015. doi:10.1016/j.jeurceramsoc.2015.08.008

[16] S. R. Levine , E. Opila , M. Halbic, J. Kisera, M. Singh, J. Salema, «Evaluation of ultra-high temperature ceramics for aeropropulsion use» *J Eur Ceram Soc*, vol. 22, pp. 2757-67, 2002. doi:10.1016/S0955-2219(02)00140-1

[17] Y. Ding, S. Dong, Q. Zhou, Z. Huang, D. Jiang, «Preparation of C/SiC composites by hot pressing, using different C fiber content as reinforcement» *J. Am. Ceram. Soc.*, vol. 89, n. 4, pp. 1447-49, 2006. doi: 10.1111/j.1551-2916.2005.00872.x

[18] V. Medri, C. Capiani, D. Gardini, «Slip casting of ZrB2–SiC composite aqueous suspensions» *ADVANCED ENGINEERING MATERIALS*, vol. 12, n. 3, pp. 210-215, 2010. doi: 10.1002/adem.200900275

[19] D. G. Munz, J. L. J. Shannon, R. T. Bubsey, «Fracture toughness calculations from maximum load in four point bend tests of chevron notch specimens» *Int. J. Fract.*, vol. 16, pp. R137-R141, 1980. doi: 10.1007/bf00013393

[20] W. G. Fahrenholtz, I. G. Hilmas, J. A. Talmy , «Refractory Diborides of Zirconium and Hafnium»

Journal American Ceramic Society, vol. 90, pp. 1347-1364, 2007. doi: 10.1111/j.1551-2916.2007.01583.x

[21] L. Zoli, D. Sciti, L.-A. Liew, K. Terauds, S. Azarnoush, R. Raj, «Additive Manufacturing of Ceramics Enabled by Flash Pyrolysis of Polymer Precursors with Nanoscale Layers» *J. Am. Ceram. Soc.*, pp. 1-7, 2015. doi: 10.1111/jace.13946

[22] L. Silvestroni, D. DalleFabbriche, C. Melandri, D. Sciti, «Relationships between carbon fiber type and interfacial domain in ZrB_2-based ceramics» *Journal of the European Ceramic Society*, vol. 36, pp. 17-24, 2016. doi:10.1016/j.jeurceramsoc.2015.09.026

[23] A. Rezaie, W. Fahrenholtz, G. E. Hilmas, «The effect of graphite addition on oxidation of ZrB2-SiC in air at 1500°C» *J. Eur. Ceram. Soc.*, vol. 33, pp. 413-421, 2013. doi:10.1016/j.jeurceramsoc.2012.09.016

[24] L. X. S. D. W. H. X. Zhang, «Crack-healing behavior of zirconium diboride composite reinforced with silicon carbide whiskers» *Scripta Mater* , vol. 59, p. 1222–5, 2008. doi:10.1016/j.scriptamat.2008.08.013